COMMUNICATION

Nitrogen-Doped Carbon Nanotube Composite Fiber with a Core–Sheath Structure for Novel Electrodes

*Tao Chen, Zhenbo Cai, Zhibin Yang, Li Li, Xuemei Sun, Tao Huang, Aishui Yu, Hamid G. Kia, and Huisheng Peng**

Carbon nanotubes (CNTs) have been recently investigated to be assembled into macroscopic fibers which may pave the way for their practical applications.[1–5] The resulting fibers maintain the remarkable mechanical and electrical properties of individual CNTs, e.g., high tensile strengths and electrical conductivities, because of the aligned structure of the building CNTs.[6,7] Therefore, they have been proposed as electrodes to fabricate a broad spectrum of optoelectronic devices such as novel organic solar cells with high performance.[8] On the other hand, certain electron-attractive elements such as nitrogen atoms have been doped into a carbon lattice of CNTs to further tune their electronic structure for desired electrocatalytic performances.[9,10] Herein, we first design and fabricate a unique core–sheath composite fiber with a core of aligned undoped CNTs with a sheath of network-like nitrogen-doped carbon nanotubes (NCNTs). The excellent 3D hopping conduction of the aligned undoped CNTs and the electrocatalytic property of the NCNT network are well combined and extend through the above structure, which provides them with unexpectedly good performance in a wide variety of application fields such as metal-free electrocatalysis of dioxygen electroreduction (DE) and sensitive detection of hydrogen peroxide.[11–13] The current density of the composite fiber electrodes for DE easily reached 2.2 mA cm^{-2} at –0.35 V in O_2-saturated 0.1 M potassium hydroxide, compared with 0.45 mA cm^{-2} at –0.05 V for a platinum wire-based electrode and is comparative to a CNT/platinum-based electrode under the same conditions.[11,13] The sensitivity of the composite fiber electrode for the detection of hydrogen peroxide is much higher than an undoped CNT fiber electrode and a NCNT-modified glassy carbon electrode. Furthermore, these composite fibers can be easily scaled up with low cost and high efficiency, and may represent a family of new fiber-shaped weavable electrodes for various electronic devices.

Fabrication of the composite NCNT fibers is detailed in the Supporting Information. To summarize, CNT arrays were first synthesized by a chemical vapor deposition process using Fe/Al_2O_3 on a silicon wafer as catalyst. Undoped CNT fibers with tunable diameters ranging from 6 to 20 μm could then be spun from the array with a thickness of ≈400 μm (see Figure S1, Supporting Information). $FeCl_3$ particles were finally coated onto undoped CNT fibers to induce growth of NCNTs on their outer surfaces at 900 °C (see Figures S2–S5, Supporting Information). **Figure 1**a shows a scanning electron microscopy (SEM) image of an undoped CNT fiber with a diameter of ≈15 μm. As shown in Figure 1d, CNTs in the fiber are highly aligned with each other and enable excellent mechanical strength, electrical conductivity, and other properties. The fiber diameter is uniform along the axial direction. Figure 1b shows a SEM image of an as-synthesized composite fiber with NCNTs in the outer hairy sheath. The core–sheath composite fiber is estimated to be ≈25 μm in diameter, so the thickness of the sheath may be calculated as 5 μm. The NCNTs further shrank to a thickness of ≈2.5 μm after treatment in a solvent such as *N*,*N*-dimethylformamide (Figure 1c). During the above process, the NCNTs lie down to form a network structure on the outer surface of the composite fiber (Figure 1e). Both the undoped CNTs and composite NCNT fibers were flexible, and could be easily bent to form coils or woven into textile electronics while maintaining the structural integrity and excellent properties (see Figure 1f,g).

Figure 2a shows a high-resolution transmission electron microscopy (TEM) image of a typical undoped CNT. The undoped CNT diameters varied between 8 and 12 nm. Figure 2b exhibits a TEM image of NCNTs with a typical bamboo-like structure, and their diameters range from 40 to 110 nm. Nitrogen contents in the NCNTs were calculated to be 4.7–5.8 wt% from energy-dispersive X-ray spectroscopy (see Table S1, Supporting Information). Note that the iron content was very low in the NCNTs, i.e., 0.02–0.06 wt%, so the as-synthesized composite fibers were directly used for DE characterization without further purification. The structures of undoped CNTs and NCNTs were further characterized by Raman spectroscopy (Figure 2c). The intensity ratio of the D-band to G-band is calculated to be 0.67 for the CNTs, and increased to 0.74 for the NCNTs because nitrogen atoms are incorporated into the carbon lattice (see Table S2, Supporting Information).

CNT fibers exhibit excellent mechanical and electrical properties. The specific strength and stiffness of these fibers are much higher than current engineering fibers.[2,4] For instance,

T. Chen, Z. Cai, Z. Yang, Dr. L. Li, X. Sun, Prof. H. Peng
Key Laboratory of Molecular Engineering of Polymers of Ministry of Education
Department of Macromolecular Science
Laboratory of Advanced Materials
Fudan University
Shanghai 200438, P. R. China
E-mail: penghs@fudan.edu.cn
Dr. T. Huang, Prof. A. Yu
Department of Chemistry and Shanghai Key Laboratory of Molecular Catalysis and Innovative Materials
Fudan University
Shanghai 200433, P. R. China
Dr. H. G. Kia
Chemical Sciences and Materials Systems Lab
GM Global R&D, 30500 Mound Road, Warren, MI 48090, USA

DOI: 10.1002/adma.201102200

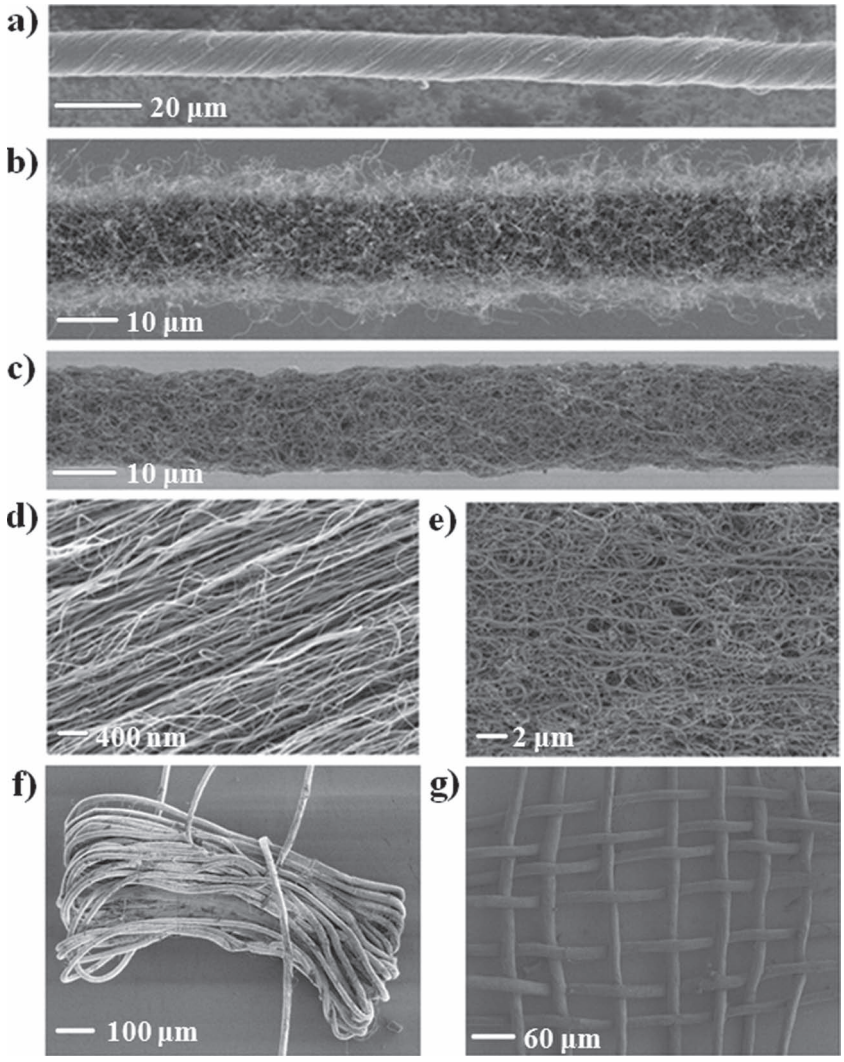

Figure 1. SEM images of undoped CNT and composite NCNT fibers. a) An undoped CNT fiber. b) An as-synthesized composite NCNT fiber. c) A composite NCNT fiber after being concentrated in *N*,*N*-dimethylformamide. d) Higher magnification of (a). e) Higher magnification of the NCNTs in (c). f) A CNT fiber being bent to form a bundle. g) A textile woven from CNT fibers.

the specific strength can be 5.3 times that of T1000 (the strongest commercial fiber), and the specific stiffness may be 4.3 times that of M70J (the stiffest commercial fiber).[2,8] The electrical conductivity of a CNT fiber can reach 400 S cm^{-1} or more at room temperature. Both mechanical strengths and electrical conductivities of our CNT fibers are comparative with those reported.[2,6] In addition, the conductivities increase with increasing temperature, indicating a semiconducting behavior (**Figure 3**b). Two main conduction mechanisms were suggested for the above temperature dependence of conductivity, i.e., a variable range hopping mechanism and a tunneling conduction mechanism.[4–6,11] Therefore, we compared the degrees of linearity for two plots of ln σ versus $T^{-1/4}$ according to the equation $\sigma = \sigma_0 \exp(-A/T^{-1/4})$ for the variable range hopping mechanism and ln σ versus $T^{-1/2}$ according to the equation of $\sigma = \sigma_0 \exp(-B/T^{-1/2})$ for the tunneling conduction mechanism. Here σ is the conductivity, σ_0, A, and B are constants, and T is temperature. The linearity degree in the variable range hopping mechanism was higher than that in the tunneling conduction mechanism, which demonstrates that the CNT fibers follow a hopping conduction mechanism. Furthermore, according to the hopping conduction equation of $\sigma \propto \exp(-A/T^{[1/(d+1)]})$, where A is a constant and d is dimensionality, we scaled conductivity with temperature by plotting ln σ versus $T^{-1/2}$ (for $d = 1$), $T^{-1/3}$ (for $d = 2$), and $T^{-1/4}$ (for $d = 3$).[3] It was found that 3D linear fitting coefficients were much higher than those in the case of one and two dimensions (Figures S6,S7, Supporting Information). These results indicate that electrical conduction in CNT fibers is dominated by a 3D hopping model.[5–8] That is, electrons hop from a CNT to neighboring ones in a fiber, which is critical for application as electrodes (Figure S8, Supporting Information).[8]

A high-efficiency electrocatalyst plays a key role for the DE in fuel cells or other electrochemical devices.[12,13] Currently, the most explored electrode catalysts for DE are fabricated from platinum or platinum alloys on carbon black, but the high cost

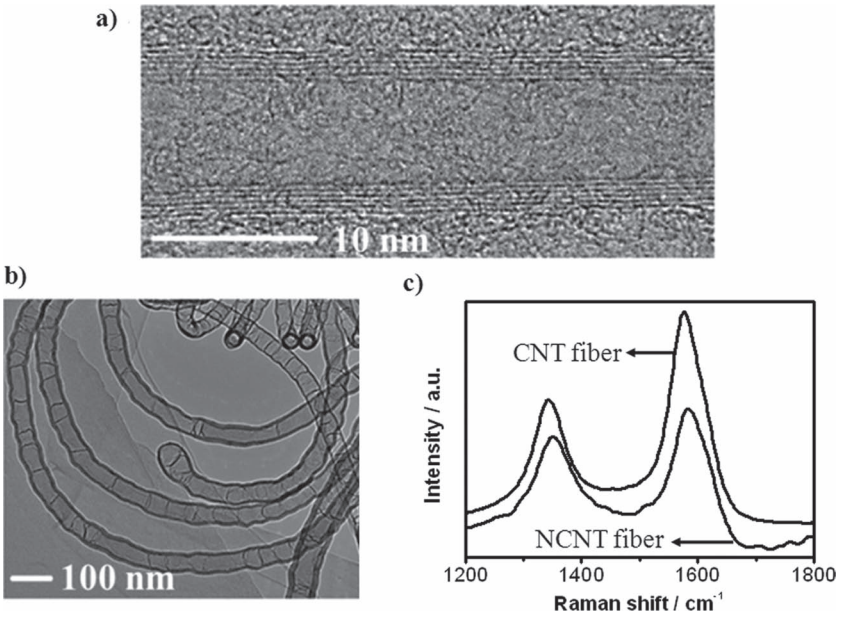

Figure 2. TEM and Raman spectroscopy characterization of CNTs and NCNTs. a) TEM image of a CNT. b) TEM image of NCNTs. c) Raman spectra of CNT and NCNT composite fibers.

of the requisite noble metal has greatly limited their large-scale applications.[14–17] In addition, platinum-based electrodes suffer from low tolerance against methanol crossover as well as susceptibility to time-dependent drift and carbon monoxide deactivation.[13] It is becoming urgent to find a material to replace platinum. Among the investigated non-platinum systems, CNTs, in particular NCNTs, show a high electrochemically accessible area with excellent electrical property and solvent resistance, which make them promising candidates for low-cost, high-efficiency, and environmentally benign non-platinum electrodes.[13,18–21] However, the application of CNTs or NCNTs as electrodes for DE has been limited by their complex fabrication because of their poor solubility and low performance because of their random dispersion. At this point, the composite NCNT fiber exhibits unique advantages and promise as an electrocatalyst for DE. Figure 3c schematically shows the growth of a NCNT composite fiber and the electrocatalytic activity.

In order to investigate the electrocatalytic activity of the composite fiber for DE, cyclic and linear sweep voltammograms in alkaline solution were performed. A CNT fiber or composite NCNT fiber, a platinum wire, a Ag/AgCl electrode (filled with saturated KCl aqueous solution), and 0.1 M KOH aqueous solution were used as working electrode, counter electrode, reference electrode, and electrolyte, respectively. The detailed fabrication of a device is shown in Figure S9, Supporting Information, and an undoped CNT fiber was studied as a comparison. Two typical reduction models had been proposed for DE in alkaline conditions.[22] The first model is characteristic of a two-step, two-electron pathway with HO_2^- and OH^- as intermediate and final products,

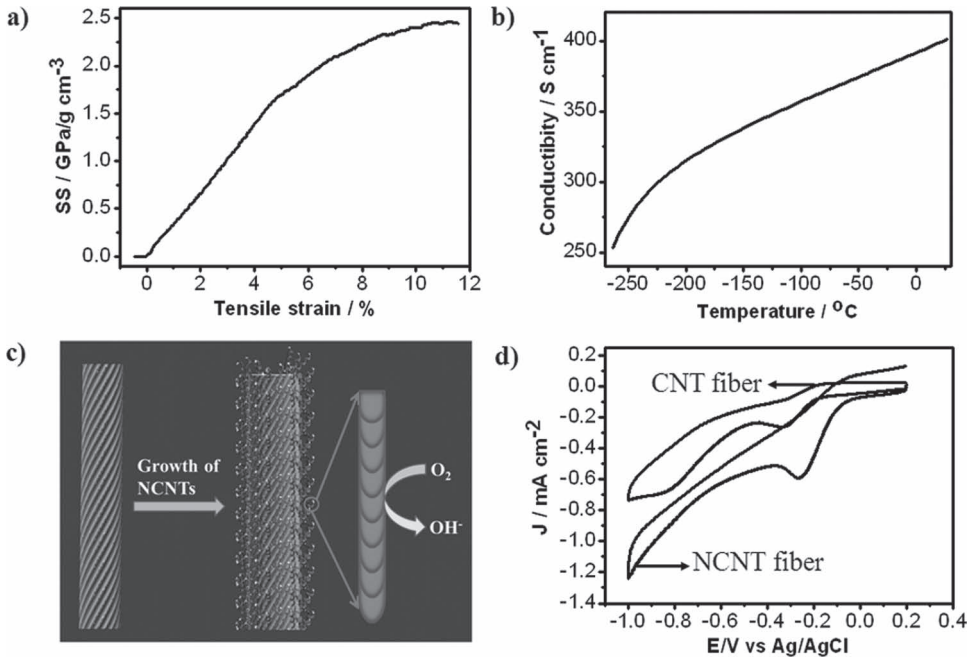

Figure 3. Mechanical, electrical, and electrocatalytic properties of undoped CNT and composite NCNT fibers. a) Specific stress (SS)–strain curve of a CNT fiber. b) The dependence of electrical conductivity on temperature of a CNT fiber measured by a four-probe method. c) Schematic illustration for the growth of NCNTs on a pure CNT fiber and the electrocatalytic activity. d) Cyclic voltammograms of pure CNT and composite fibers in air-saturated 0.1 M KOH aqueous solution both with a scan rate of 100 mV s^{-1}.

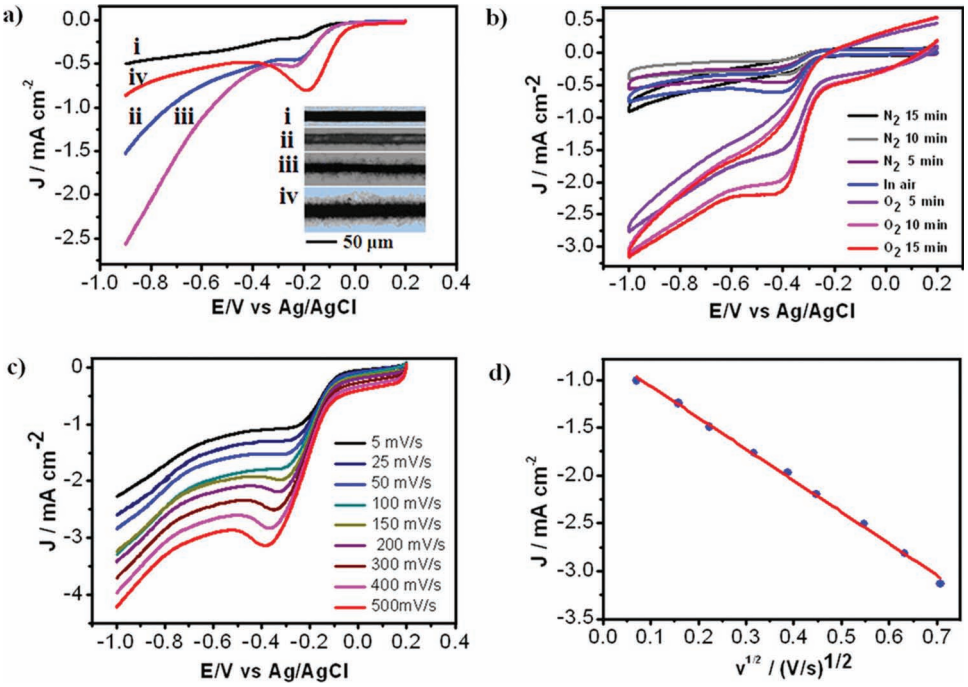

Figure 4. Electrocatalytic properties of composite NCNT fibers. a) Linear sweep voltammograms of composite fibers with different NCNT densities in air-saturated 0.1 M KOH aqueous solution with a scan rate of 100 mV s^{-1} (the insets show optical images of the composite fibers with growth times of 0, 1, 5, and 10 min for i, ii, iii, and iv, respectively). b) Cyclic voltammograms of a composite fiber under different oxygen partial pressures. c) Linear sweep voltammograms of a composite fiber in O_2-saturated 0.1 M KOH aqueous solution with different scan rates. d) Plot of the peak DE current density versus square root of the scan rate (v).

respectively. For the second model, a more efficient four-electron process occurs with water as the final product. Figure 3d shows a typical cyclic voltammogram of an undoped CNT fiber with two reduction peaks at –0.32 and –0.83 V, which suggests a two-electron model in the DE. The reduction peak at –0.32 V is attributed to the reduction process from O_2 to HO_2^- which is electrochemically mediated by the oxygen-containing groups, while the peak at –0.83 V corresponds to the reduction of HO_2^- to OH^-.[23,24]

However, compared with undoped CNT fibers, only a sharp reduction peak at a higher potential of –0.26 V was observed for composite NCNT fibers, which agrees more with a four-electron reduction model for the DE.[24,25] The DE peak of the composite NCNT fiber significantly shifts about 60 mV to the positive potential compared to undoped CNT fibers. That is, the composite NCNT fibers show a much improved catalytic activity for DE as the positive potential is kinetically more favorable. In addition, it was also shown that the current density increased at least two times in the composite fiber compared to the undoped CNT fiber (see Figure S10, Supporting Information). For both undoped CNT and composite NCNT fibers, no characteristic electrocatalytic peaks at around –1.0 and –0.65 V for iron had been found,[26] which agrees with the energy-dispersive X-ray spectroscopy analysis. Therefore, the electrocatalytic performance mainly originates from the NCNTs in the composite fibers and not as a result of trace iron. The above conclusion has been further confirmed by the fact that current densities increase with increasing NCNT contents. The NCNT contents can be easily tuned by a number of catalyst particles which control the NCNT densities and growth time, which determines their lengths. For instance, **Figure 4**a shows that the current densities increased with increasing growth times of NCNTs. At present, the DE current density of the composite NCNT fiber easily achieves 2.2 mA cm^{-2} at –0.35 V in O_2-saturated 0.1 M potassium hydroxide, compared with 0.45 mA cm^{-2} at –0.05 V for a platinum-based three-electrode system under the same conditions (see Figure S11, Supporting Information), and comparative to a CNT/platinum-based electrode. The current density may be further improved by optimizing fiber structures. It should be noted that rotating ring-disk electrode experiments are generally used to study the DE process. However, the structures of the composite NCNT fibers were varied during preparation for the test. Further investigation is required to confirm their four-electron reduction behavior.

Several important factors contribute to the high electrocatalytic performance of composite NCNT fibers. Firstly, the electron-accepting nature of the nitrogen atoms produces positive charges in neighboring carbon atoms to attract electrons from the anode.[18,19] Secondly, the high specific surface area of the NCNT network in the fiber sheath greatly increases their interactions with the electrolyte solution. Thirdly, the fiber core composed of aligned CNTs exhibits a 3D hopping conduction mechanism, and the charges on the outer surface are efficiently transferred to an external circuit. Therefore, the produced charges in the NCNTs could be immediately and efficiently transported from the NCNTs to the CNTs. In particular, the high interfacial area between the NCNTs and CNTs enhances the transfer efficiency.

In order to further identify the DE signals of composite fibers, a series of cyclic voltammograms were obtained by varying the oxygen concentration in the electrolyte solution which was controlled by changing O_2 partial pressures. Figure 4b shows that the composite fiber electrode was highly sensitive to oxygen concentration. The current densities increased with increasing oxygen concentrations, and reached a steady value of 2.2 mA cm^{-2} after O_2 was passed through the electrolyte solution for 15 min or longer (O_2 in a saturated state). The DE on a composite fiber is further performed at different scan rates (Figure 4c). Figure 4d shows a perfect straight line of peak currents for DE versus the square root of the potential scan rate, which indicates that oxygen reduction at the composite fiber electrode is a diffusion-controlled process.

Because of their excellent mechanical, electrical, and thermal properties, the composite NCNT fibers showed good stability as DE electrodes. For instance, chronoamperometric responses in a 0.1 M KOH aqueous solution at –0.25 V showed that current densities tended to be stable at ≈1.0 mA cm^{-2} during a prolonged time (Figure S12, Supporting Information). In addition, NCNTs had been exhibited to maintain the same amperometric responses without crossover and poison effects in the presence of fuel molecules such as hydrogen gas, glucose, methanol, formaldehyde, and carbon monoxide. As a comparison, commercial platinum-based electrodes deteriorated in electrocatalytic activity after cycling and easily succumbed to crossover and poison effects.[13]

Composite NCNT fibers are also promising for a wide variety of sensing applications such as the detection of H_2O_2 based on their excellent electrocatalytic properties. H_2O_2 is often produced by enzymatic reactions between oxidase and their substrates, so substrates may be easily detected by monitoring the concentration of regenerated H_2O_2. Because of its high sensitivity and low cost, the electrochemical detection of H_2O_2 plays a critical role in bio-sensing fields, e.g., food, pharmaceutical, and environmental analysis.[27] Here the oxidation of H_2O_2 may be considered as a reverse process of a oxygen reduction reaction where O_2 reduces to H_2O_2. **Figure 5**a shows a typical current–time curve of a composite NCNT fiber electrode for successive addition of H_2O_2 in phosphate buffer solution at +0.3 V (Ag/AgCl as reference electrode). Oxidation currents obviously rise and reach a stable value in less than 2 s with continuous addition of H_2O_2 to the buffer solution. In addition, the currents are proportional to H_2O_2 concentrations at a range of 1×10^{-3} to 7×10^{-3} M with a correlation coefficient of 0.9937 (Figure 5b). The sensitivity is calculated as 1.0×10^3 μA M^{-1}, which is much higher than an undoped CNT fiber electrode (0.20×10^3 μA M^{-1} in Figure S13, Supporting Information) and a NCNT-modified glassy carbon electrode (0.03×10^3 μA M^{-1}).[28]

To further evaluate the sensing reproducibility and stability of the NCNT composite fiber, current–time curves were carefully traced for different cycling times. One cycle was realized after alternate sensing and washing operations, and H_2O_2 was removed during the washing process. It was found that these sensors based on NCNT composite fibers can effectively recover after the sensing event many times. For instance, Figure S14, Supporting Information, compares current–time curves of a NCNT composite fiber sensor which was performed in 50×10^{-3} M phosphate buffered saline solution (pH = 7.4) after successive addition of 1×10^{-3} and 10×10^{-3} M H_2O_2 during the first and fifth sensing cycles. The two responding curves are almost the same. It should also be noted that such sensors maintained the same sensing capability to H_2O_2 after exposure to air for months. These results indicate a good sensing reproducibility and stability of the NCNT composite fiber.

In summary, we have designed and fabricated a novel core–sheath composite fiber of which the core and the sheath are composed of aligned CNTs and network-like NCNTs, respectively. These composite fibers are flexible and weavable with excellent mechanical and electrical properties, which make them very promising as a family of new and high-performance fiber-shaped electrodes for DE, hydrogen peroxide sensing, and various other electronic devices.

Experimental Section

CNT arrays were synthesized by a chemical vapor deposition in a quartz tube furnace using Fe (1 nm)/Al_2O_3 (10 nm) on silicon wafer as the catalyst, ethylene as the carbon source, and a mixture of Ar and H_2 gases as the carrying gas typically at 750 °C. Pure CNT fibers were then spun from the arrays. Figure S1, Supporting Information, shows an optical microscopy image of the spinning process of a CNT array

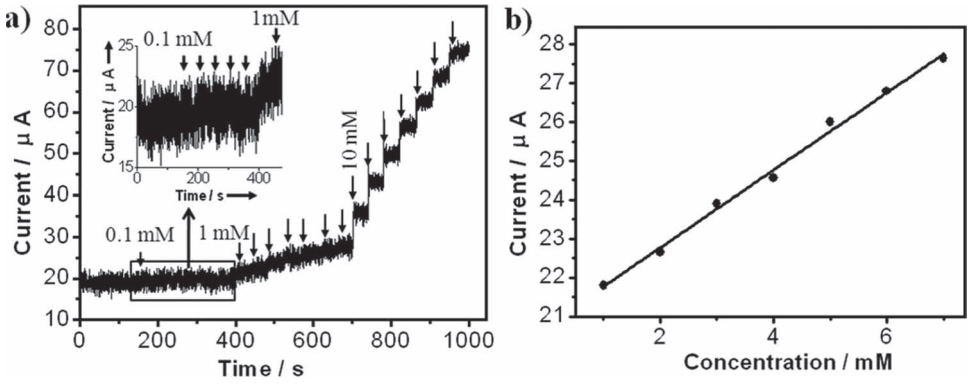

Figure 5. Composite NCNT fiber as an electrode for the sensitive detection of H_2O_2. a) Current–time curve of a composite fiber electrode with successive addition of H_2O_2 (indicated by arrows with marked concentrations) to a buffer solution at +0.30 V versus Ag/AgCl. b) Linear relationship between the current of the fiber electrode and the concentration of added H_2O_2 (correlation coefficient of 0.9937).

to form a fiber through the use of a rotating microprobe. The rotation speeds of the microprobe ranged from 1000 to 3000 rad min^{-1} during the fiber spinning.[2,6] CNT fibers were assembled into textiles according to a typical weaving process of general chemical fibers.

The growth of NCNTs on the pure CNT fiber is schematically shown in Figure S2, Supporting Information. Firstly, $FeCl_3$ was coated onto the pure CNT fiber by immersing it in a 0.1 M $FeCl_3$ aqueous solution, followed by evaporation of water. The resulting fiber was placed in a tube furnace to grow NCNTs, and a mixture of Ar (560 sccm) and H_2 (35 sccm) was used as the carrying gas. The detailed temperature changes during the growth are shown in Figure S3, Supporting Information. To summarize, the furnace temperature was increased from room temperature to 900 °C in ≈20 min and maintained at 900°C for ≈40 min to reduce $FeCl_3$ to Fe under the carrying gas. Ethylenediamine was then introduced into the furnace as the carbon and nitrogen sources to grow NCNTs for ≈20 min. The growth was completed by stopping the ethylenediamine and decreasing the furnace temperature to room temperature.

The fabrication and setup of a three-electrode system to characterize the electrocatalytic property of the pure CNT or composite fibers are schematically shown in Figure S9, Supporting Information. A pure CNT or composite fiber was first transferred to a clean glass slide with one end stabilized by silver paste and connected to a silver wire. The pure CNT or composite fiber was used as a working electrode with a platinum wire counter electrode, a Ag/AgCl (filled with saturated KCl aqueous solution) reference electrode, and a 0.1 M KOH aqueous solution as electrolyte. Note that the silver paste at one end of the fiber should not be immersed in the electrolyte solution when the other end is immersed into the solution during the cell assembly, because silver paste may affect the DE. The produced current densities of the composite fibers were calculated from the ratio between the steady state current obtained from the DE curve and the efficient geometric area of the fiber. A phosphate buffer solution (Na_2HPO_4/KH_2PO_4) with a concentration of 50×10^{-3} M (pH = 7.4) was used as the electrolyte for sensitive detection of H_2O_2. The surface areas of the fiber electrodes were calculated from their geometric areas.

The structures of CNTs and NCNTs were characterized by TEM (JEOL JEM-2100F operated at 200 kV) and SEM (Hitachi FE-SEM S-4800 operated at 1 kV). TEM samples were prepared by drop-casting *N*,*N*-dimethylformamide solutions of CNTs or NCNTs onto copper grids in the open air. The optical microscopy images were taken using an Olympus BX52. Mechanical tests were performed using a Shimadzu Table-Top Universal Testing Instrument. The used fiber was mounted on a paper tab with a gauge length of 5 mm, and the fiber diameter was measured by SEM. Raman measurements were performed on a Renishaw inVia Reflex with an excitation wavelength of 514.5 nm and a laser power of 20 mW at room temperature. The electrical conductivities were characterized by a physical property measurement system through a four-probe method. The cyclic and linear voltammograms, and sensitive detection of hydrogen peroxide, were performed on a CHI 660a electrochemical workstation (Shanghai, China) at room temperature. The oxygen concentrations in the electrolyte solution were varied by changing the purging times of O_2 or N_2. The gases were introduced and released through a gas inlet and a gas outlet on the top of the electrochemical cell, respectively.

Supporting Information

Supporting Information is available from the Wiley Online Library or from the author.

Acknowledgements

This work was supported by Natural National Science Foundation of China (20904006, 91027025), Ministry of Science and Technology (2011CB932503, 2011DFA51330), Science and Technology Commission of Shanghai Municipality (1052nm01600, 09PJ1401100), Program for New Century Excellent Talents in University (NCET-09-0318), Ministry of Education of China, General Motors Company, Li Foundation Heritage Prize, and Program for Key Discipline Creativity Talents at Fudan University.

Received: June 12, 2011
Revised: July 21, 2011
Published online: September 12, 2011

[1] a) K. Jiang, Q. Li, S. Fan, *Nature* **2002**, *419*, 801; b) M. Zhang, K. R. Atkinson, R. H. Baughman, *Science* **2004**, *306*, 1358.
[2] X. Zhang, Q. Li, T. G. Holesinger, P. N. Arendt, J. Huang, P. D. Kirven, T. G. Clapp, R. F. DePaula, X. Liao, Y. Zhao, L. Zheng, D. E. Peterson, Y. Zhu, *Adv. Mater.* **2007**, *19*, 4198.
[3] Q. Li, Y. Li, X. Zhang, S. B. Chikkannanavar, Y. Zhao, A. M. Dangelewicz, L. Zheng, S. K. Doorn, Q. Jia, D. E. Peterson, P. N. Arendt, Y. Zhu, *Adv. Mater.* **2007**, *19*, 3358.
[4] K. Koziol, J. Vilatela, A. Moisala, M. Motta, P. Cunniff, M. Sennett, A. Windle, *Science* **2007**, *318*, 1892.
[5] H. Peng, M. Jain, Q. Li, D. E. Peterson, Y. Zhu, Q. Jia, *J. Am. Chem. Soc.* **2008**, *131*, 1130.
[6] H. Peng, X. Sun, F. Cai, X. Chen, Y. Zhu, G. Liao, D. Chen, Q. Li, Y. Lu, Y. Zhu, Q. Jia, *Nat. Nanotechnol.* **2009**, *4*, 738.
[7] H. Peng, M. Jain, D. E. Peterson, Y. Zhu, Q. Jia, *Small* **2008**, *4*, 1964.
[8] T. Chen, S. Wang, Z. Yang, Q. Feng, X. Sun, L. Li, Z. Wang, H. Peng, *Angew. Chem. Int. Ed.* **2011**, *50*, 1815.
[9] D. L. Carroll, Ph. Redlich, X. Blase, J.-C. Charlier, S. Curran, P. M. Ajayan, S. Roth, M. Ruhle, *Phys. Rev. Lett.* **1998**, *81*, 2332.
[10] P. Ayala, R. Arenal, A. Rubio, T. Pichler, *Carbon* **2010**, *48*, 575.
[11] N. Alexeyeva, K. Tammeveski, A. Lopez-Cudero, J. Solla-Gullón, J. M. Feliu, *Electrochim. Acta* **2011**, *55*, 794.
[12] B. Wang, *J. Power Sources* **2005**, *152*, 1.
[13] K. Gong, F. Du, Z. Xia, M. Durstock, L. Dai, *Science* **2009**, *323*, 760.
[14] J. Zhang, K. Sasaki, E. Sutter, R. R. Adzic, *Science* **2007**, *315*, 220.
[15] B. Lim, M. J. Jiang, P. H. C. Camargo, E. C. Cho, J. Tao, X. M. Lu, Y. M. Zhu, Y. N. Xia, *Science* **2009**, *324*, 1302
[16] N. Tian, Z.-Y. Zhou, S.-G. Sun, Y. Ding, Z. L. Wang, *Science* **2007**, *316*, 732.
[17] T. C. Nagaiah, S. Kundu, M. Bron, M. Muhler, W. Schuhmann, *Electrochem. Commun.* **2010**, *12*, 338.
[18] W. Xiong, F. Du, Y. Liu, A. Perez, Jr., M. Supp, T. S. Ramakrishnan, L. Dai, L. Jiang, *J. Am. Chem. Soc.* **2010**, *132*, 15839.
[19] D. Yu, Q. Zhang, L. Dai, *J. Am. Chem. Soc.* **2010**, *132*, 15127.
[20] S. Yang, G.-L. Zhao, E. Khosravi, *J. Phys. Chem. C* **2010**, *114*, 3371.
[21] M. D. Lima, S. Fang, X. Lepró, C. Lewis, R. Ovalle-Robles, J. Carretero-González, E Castillo-Martínez, M. E. Kozlov, J. Oh, N. Rawat, C. S. Haines, M. H. Haque, V. Aare, S. Stoughton, A. A. Zakhidov, R. H. Baughman, *Science* **2011**, *331*, 51.
[22] Y. Shen, M. Träuble, G. Wittstock, *Anal. Chem.* **2008**, *80*, 750.
[23] M. Zhang, Y. Yan, K. Gong, L. Mao, Z. Guo, Y. Chen, *Langmuir* **2004**, *20*, 8781.
[24] K. Gong, P. Yu, L. Su, S. Xiong, L. Q. Mao, *J. Phys. Chem. C* **2007**, *111*, 1882.
[25] N. Alexeyeva, E. Shulga, V. Kisand, I. Kink, K. Tammeveski, *J. Electroanal. Chem.* **2010**, *648*, 169.
[26] U. Casellato, N. Comisso, G. Mengoli, *Electrochim. Acta* **2006**, *51*, 5669.
[27] X. Xu, S. Jiang, Z. Hu, S. Liu, *ACS Nano* **2010**, *4*, 4292
[28] Y. Tang, B. L. Allen, D. R. Kauffman, A. Star, *J. Am. Chem. Soc.* **2009**, *131*, 13200.